

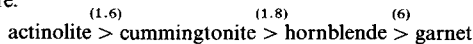
Mg-Fe-Mn distribution in amphiboles, pyroxenes, and garnets and implications for conditions of metamorphism of high-grade early Archaean iron-formation, southern West Greenland

R. P. HALL

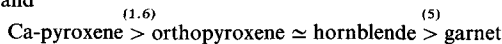
Department of Geology, Portsmouth Polytechnic, Burnaby Road, Portsmouth PO1 3QL

ABSTRACT. Remnants of early Archaean (Akilia) iron-formation occur as enclaves within the c. 3700 Ma Amitsoq gneisses in the eastern Godthåb-Sukkertoppen region of southern West Greenland. Amphibole- and pyroxene-bearing assemblages are preserved respectively in these two areas. The amphibole-facies rocks comprise one, two, and three-amphibole-bearing assemblages, co-existing with magnetite and quartz (and locally garnet). Experimentally determined phase equilibria suggest that the amphibole-bearing types have not exceeded c. 700 °C, while distribution coefficients in the two-pyroxene iron-formation indicate a maximum temperature of around 625 °C.

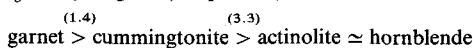
Mg-Fe distribution relationships between the phases are:



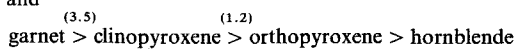
and



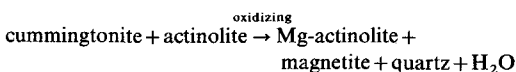
where the numbers are generalized distribution coefficients ($K_{D(Mg)}^{a,b} = [X_{Mg}^a/(1-X_{Mg}^a)]/[X_{Mg}^b/(1-X_{Mg}^b)]$ and $X_{Mg}^a = \text{Mg}/(\text{Mg} + \text{Fe})$ in phase *a*). Mn distribution is:



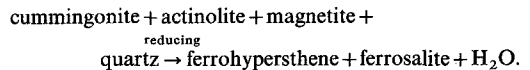
and



($Y_{Mn} = 0$) where $K_{D(Mn)}^{a,b} = Y_{Mn}^a/Y_{Mn}^b$ and $Y_{Mn} = \text{Mn}/(\text{Mn} + \text{Mg} + \text{Fe})$. The distribution coefficients are variable both from one rock to another and internally from one set of grain pairs to another. The development of the observed variable silicate phase assemblages is dependent upon a complex interaction of not only metamorphic grade (*P* and *T*) and element availability, but more importantly a_{H_2O} and f_{O_2} . In particular, the possibility of reactions between observed assemblages containing cummingtonite + actinolite, magnesian actinolite + magnetite and ferropargasite + ferrosalite suggest lesser or greater degrees of dehydration under oxidizing or reducing conditions. For example:



and



KEYWORDS: amphiboles, pyroxenes, garnets, metamorphism, iron-formation, SW Greenland.

IRON-FORMATION is one of the most characteristic lithologies of the oldest group of Archaean rocks (the Akilia association) in southern West Greenland (McGregor and Mason, 1977). It forms a large unit of the Isua supracrustal belt at Isukasia (fig. 1) which has yielded an isotopic age of c. 3770 Ma (Moorbath *et al.*, 1977; Hamilton *et al.*, 1983). This belt is a continuous horizon approximately 1 km thick surrounded by Amitsoq gneisses (c. 3700 Ma) and relict intrusive contacts are locally preserved between these two units (Nutman *et al.*, 1983). Elsewhere, the Akilia rocks are variably preserved as smaller horizons and inclusions within the Amitsoq gneisses.

Amitsoq gneisses occupy the NE corner of the Ivisártoq area (fig. 1), the geology of which has been described elsewhere (Hall, 1981; Hall and Friend, 1983). The area is dominated by a large belt of Malene supracrustal rocks (Table I), comprising various semipelitic, quartz-rich and carbonate-rich paragneisses, ultrabasic lenses and metavolcanic amphibolites (Hall, 1980). Mineral assemblages in these rocks and the enveloping younger Nùk-type gneisses indicate that they attained upper amphibolite facies conditions (Hall, 1981).

No iron-formation has been recognized among any of the Malene-type supracrustal rocks of the region, and hence enclaves of iron-formation suggest the presence of pre-Amitsoq material in the granulite-facies terrain of the Qardlît taserssuat lake area, east of Sukkertoppen (Hall, 1978, 1981). These enclaves are thought to represent the few

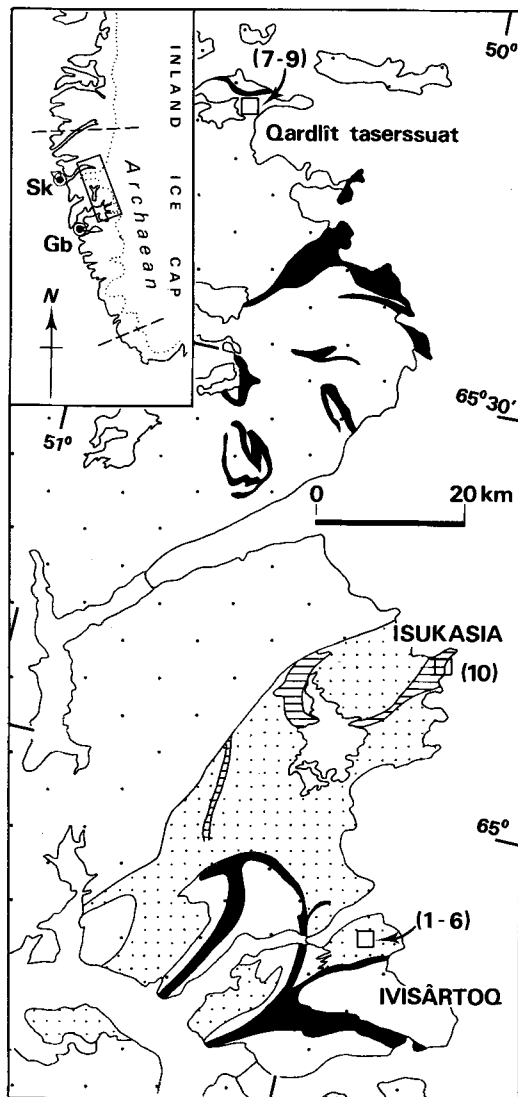


FIG. 1. Simplified geological sketch map of the eastern Godthåb-Sukkertoppen region showing localities of samples 1 to 10 and distribution of major occurrences of pre-Amitsoq (Akilia/Isua) supracrustal rocks (horizontal line shading), Amitsoq gneiss (stippled), Malene supracrustal rocks (black) and Nûk-type gneiss (light stipple) (after compilation by Allaart, 1982). The inset map of southern West Greenland depicts the extent of the map area within the Archaean craton, and the location of Godthåb (Gb) and Sukkertoppen (Sk).

relict resistors after the overwhelming invasion by Nûk-type granitic material (cf. Hall and Friend, 1983). A full account of the Archaean complex of the region is presented by Bridgwater *et al.* (1976)

TABLE I. Principal lithostratigraphic units of the Archaean complex of southern West Greenland*.

Qôrqt granite complex (c. 2500 Ma).
Nûk-type tonalitic - granitic gneisses (<c. 3000 Ma)
Malene supracrustal suite
Ameralik basic dykes
Amitsoq tonalitic - granitic gneisses (c. 3600 Ma)
Akilia (Isua) supracrustal rocks (c. 3770 Ma)

* Generalised isotopic age data from Moorbath *et al.* (1977; 1981), Taylor *et al.* (1980) and Hamilton *et al.* (1983).

and a 1:500 000 scale geological map has been compiled by Allaart (1982).

Iron-formation samples. Six samples of iron-formation from enclaves within the Amitsoq gneisses of Ivisártoq and three samples from the Qardlit taserssuat lake area (fig. 1) have been examined. The composition of these samples has been determined by wet chemical analysis techniques at the Departments of Geology of Portsmouth Polytechnic and the University College of Wales, Aberystwyth, and has been confirmed by combined mineral chemistry and modal analysis. Selected chemical analyses are presented in Table II, and full geochemical data are presented by Hall (1981).

The samples from Ivisártoq (samples 1-6) are all amphibole-bearing. Of these, two comprise a three-amphibole assemblage (cummingtonite + actinolite + hornblende), two contain two amphiboles (cummingtonite + actinolite) and two carry only actinolite, all coexisting with magnetite and quartz (Table II). Neither pyroxene nor fayalite occurs in any of these samples. Almandine garnet occurs as an accessory phase in samples 2 and 3. Three, different intercalated iron-formation lithologies occur in the Qardlit taserssuat area (samples 7-9). These are a cummingtonite + actinolite-bearing rock, very similar to the Ivisártoq samples, a two-pyroxene + hornblende + garnet type and a quartz + almandine garnet lithology. One sample (10) from Isukasia (fig. 1) has been examined. The iron-formation in this area retains a millimetre-scale quartz-magnetite (and locally hematite) banding (fig. 2a), and actinolite and (more rarely) cummingtonite occur as small acicular grains in the quartz-rich bands of the examined sample. The Ivisártoq and Qardlit taserssuat samples are coarser, polygonal granoblastic textured rocks in which the original fine banding is obscured to a large extent (fig. 2b). Representative analyses are

TABLE II. Modal and chemical composition of iron-formation enclaves from Ivisártoq (1-6) and eastern Sukkertoppen (7-9).

Sample	1.	2.	3.	4.	5.	6.	7.	8.	9.
CGU No	200816	200817	200821	200823	200827	200846	220512	220513	220514
quartz	56	56	67	49	76	55	43	62	38
magnetite	23	13	12	30	11	23	24	3	23
cummingtonite	-	19	-	4	8	17	-	-	11
actinolite	21	10	21	17	5	5	-	-	28
'hornblende'	-	2	-	-	tr.	-	tr.	-	-
garnet	-	tr.	tr.	-	-	-	-	30	-
orthopyroxene	-	-	-	-	-	-	32	5	-
clinopyroxene	-	-	-	-	-	-	1	-	-
apatite	tr.	tr.	-	tr.	tr.	tr.	-	-	-
rutile	-	-	tr.	-	-	tr.	-	-	tr.
epidote	-	-	tr.	-	-	-	-	-	-
wt %									
SiO ₂	55.44	62.47	68.35	52.36	72.02	51.60	48.38	67.92	47.46
Al ₂ O ₃	0.26	0.64	0.29	0.20	0.20	0.13	0.13	8.25	0.58
FeO	12.70	16.20	8.76	15.80	10.40	18.20	22.93	16.62	17.90
Fe ₂ O ₃	27.44	12.76	15.44	26.60	13.89	26.74	24.60	3.60	27.14
MgO	2.68	4.60	3.01	2.59	2.02	2.28	3.45	1.18	4.03
CaO	2.00	1.73	2.50	1.72	0.91	1.33	0.34	2.43	2.35
Na ₂ O	0.08	0.01	0.17	0.07	0.04	0.08	tr.	-	0.17
K ₂ O	0.03	0.01	0.02	0.02	0.02	0.03	tr.	-	0.15
TiO ₂	0.41	tr.	0.01	0.16	0.14	0.36	-	-	0.20
MnO	0.16	0.68	0.29	0.10	0.23	0.12	0.15	0.45	0.19
P ₂ O ₅	0.05	tr.	0.01	0.04	0.02	0.04	tr.	tr.	0.04
ppm									
Ni	9	n.a.	52	50	21	10	n.a.	n.a.	18
Zn	75	n.a.	223	122	51	111	n.a.	n.a.	207
Y	1	n.a.	5	9	-	11	n.a.	n.a.	16
Ce	6	n.a.	2	12	10	15	n.a.	n.a.	9

tr = trace; n.a. = not analysed.

CGU No is the sample number allocated by the Geological Survey of Greenland (Grønlands Geologiske Undersøgelse)

presented of cummingtonites (Table III), actinolite (Table IV) and 'hornblendes', garnets, clinopyroxene, and orthopyroxene (Table V) from the various samples.

Geochemistry. Modal and geochemical analyses of the iron-formation samples (except sample 10) are presented in Table II. As a group they show a good geochemical coherence except for sample 8 (garnet + quartz rock) which clearly represents a different, relatively Fe-poor, aluminous facies. The other eight samples are dominated by silica and iron-oxide, the contents of which vary from 47 to 72 wt. % and 24 to 47 wt. % respectively, (modal quartz and magnetite contents range from 38 to 76% and 11 to 30%, respectively). Mg and Ca constitute the bulk of the remainder, incorporated within amphiboles or pyroxenes (and locally garnet). Al, K, Na, Ti, and Mn are present in minor amounts, incor-

porated within the various silicate phases. P₂O₅ occurs in very low concentrations (0 to 0.05 wt. %), and corresponds to the accessory apatite content. The overall geochemical composition of the samples is similar to that of many other iron-formation units (Bayley and James, 1973; Beukes, 1973; Dorr, 1973). It closely resembles the composition of the samples from south of Godthåb (fig. 1) quoted by McGregor and Mason (1977) but it is more restricted than the wide geochemical range of the various iron-formation facies at Isukasia (Appel, 1980).

The concentrations of fifteen trace elements (Sc, V, Cr, Ni, Cu, Zn, Rb, Sr, Y, Zr, Nb, Ba, La, Ce, and Nd) were determined by X-ray fluorescence analysis at Portsmouth Polytechnic using the data retrieval techniques of Brown *et al.* (1973). Only Ni and Zn consistently occur in significant amounts

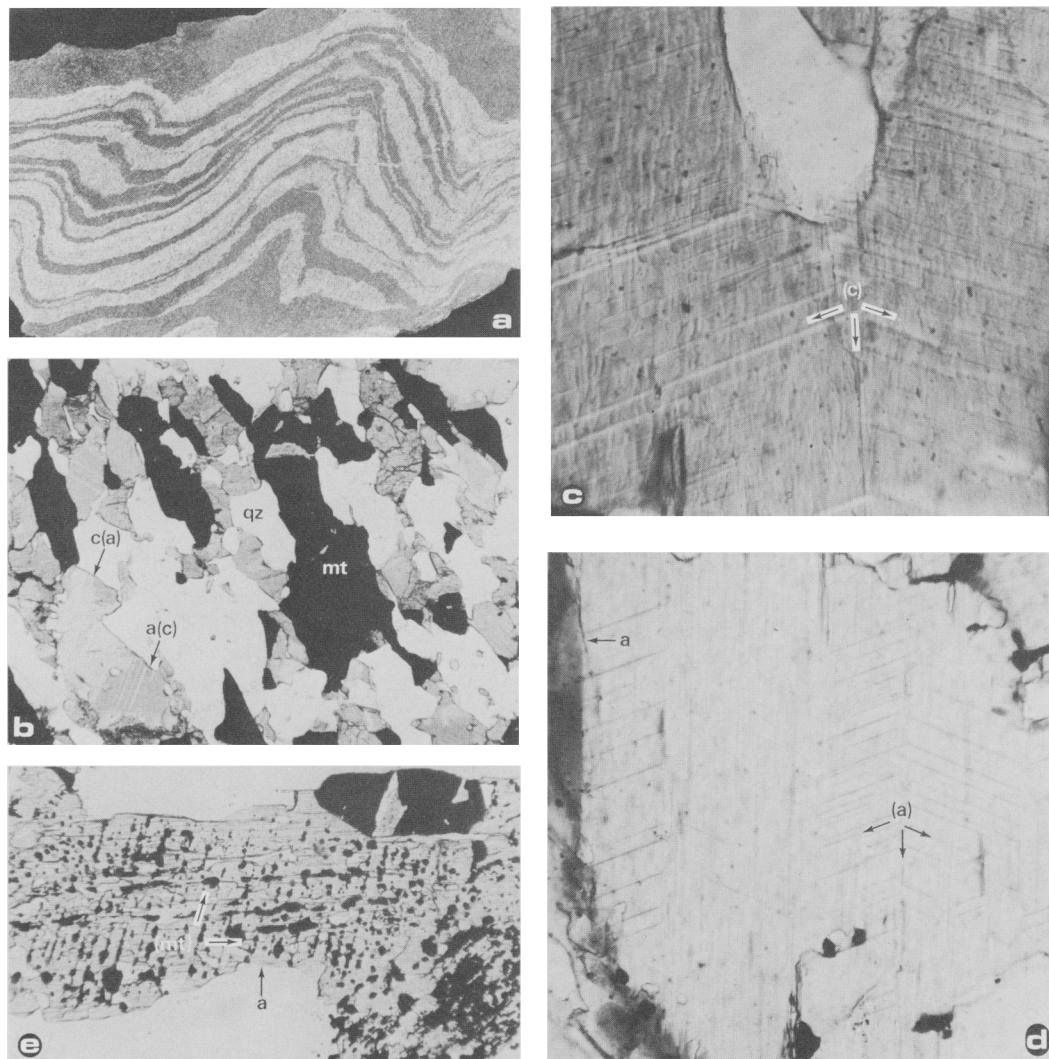


FIG. 2. (a) Relict banding preserved as quartz-rich and magnetite-rich layers in iron-formation sample 10 (GGU 213146) from Isukasia. Length of cut surface approximately 8 cm. (b) Amphibolite facies iron-formation sample 9 (GGU 220514) comprised of quartz (colourless; qz), magnetite (black; mt), actinolite (dark grey) and cummingtonite (pale grey). Fine exsolution lamellae of cummingtonite within an actinolite host [a(c)] and actinolite within a cummingtonite host [c(a)] occur separately and as single complex grains (arrowed). Field of view 3×2.3 mm (p.p.l.). (c) Fine cummingtonite lamellae [pale grey; (c)] exsolved parallel to $(\bar{1}01)$ and repeated across a (100) exsolution/twin plane in a host actinolite (dark grey) in sample 9. Field of view 0.3×0.3 mm (p.p.l.). (d) 'Herringbone' texture of fine actinolite lamellae [dark grey; (a)] exsolved parallel to $(\bar{1}01)$ and repeated across multiple (100) exsolution/twin planes in a host cummingtonite (light grey) in sample 2 (GGU 200817). Actinolite also forms a coarse margin to the grain. Field of view 0.5×0.5 mm (p.p.l.). (e) Exsolved magnetite [black; (mt)] and blebby quartz (colourless) within a host actinolite (a) of sample 1 (GGU 200816). The two exsolution planes are indicated by the arrows. Field of view 1×0.6 mm (p.p.l.).

(9–52 ppm and 51–223 ppm respectively). Most of the other trace elements are at or below the limit of detection (Table II).

The distribution of rare earth elements (REE) is

indicated by the ratio of Ce to Y. The latter element can be regarded as a heavy rare earth (erbium) proxy (Herrman, 1970). The fractionation ratio $Ce_{N_{chon}}/Y_{N_{chon}}$ varies from 0.71 to 14.1 (samples 3

and 1 respectively), where Ce_{Nchon} and Y_{Nchon} represent values normalized to those of average chondrite ($Ce = 0.87$ ppm and $Y = 1.8$ ppm). This signifies a slight relative light *REE* enrichment with absolute values of Ce between 2 and 23 times that of chondrite. Archaean sediments are known to have lower *REE* abundances than post-Archaean ones (e.g. Wildeman and Haskin, 1973; Taylor and McClennan, 1981) and the analysed iron-formation samples have even lower abundances, with slight relative heavy *REE* enrichment when normalized to typical shale values (Turekian and Wedepohl, 1961). These results are in accordance with those derived from the Godthåb and Isukasia samples (McGregor and Mason, 1977; Appel, 1980) and for similar rocks from elsewhere (e.g. Fryer, 1977; Laajoki and Lavikainen, 1977).

Silicate phases. The iron-formation samples are considered in two groups: (a) amphibole-bearing and (b) pyroxene-bearing assemblages. The former group comprises various single, two and three-amphibole varieties coexisting with quartz and magnetite: (i) actinolite (+ garnet); (ii) (ferro-) actinolite + cummingtonite (iii) actinolite + cummingtonite + ferro-hornblende (iv) actinolite + cummingtonite + ferro-hornblende + garnet (amphibole nomenclature from Leake, 1978). The Ca-poor and calcic amphiboles occur both as discrete grains and, more commonly, as exsolved pairs. There is a complete range in the proportion of Ca-poor to calcic amphibole in these pairs with both cummingtonite exsolution in host actinolite (fig. 2c) and actinolite lamellae in host cummingtonite grains (fig. 2d) occurring on fine and coarse scales (fig. 2b) along (100) and ($\bar{1}01$) planes (cf. Robinson *et al.*, 1971; Immege and Klein, 1976). A 'herringbone' texture is developed locally, where ($\bar{1}01$) lamellae are repeated across (100) twin planes along which exsolution also occurs (fig. 2c, d). The locally patchy intergrowth of the two amphiboles has probably developed by the coalescence of originally discrete lamellae (Klein, 1968; Simmons *et al.*, 1974).

The single-amphibole assemblage actinolites also show evidence of exsolution, but in this case of magnetite and to a lesser extent quartz (fig. 2e). The significance of this texture is discussed below. The pyroxene facies iron-formation sample (7) has a chemical composition very similar to the amphibole-bearing varieties (Table II). It comprises quartz + magnetite + ferropyrstherne (+ ferrosalite + ferro-hornblende). The pyroxenes show no normal exsolution textures, although some of the ferropyrstherne grains contain thin lamellae, apparently of clinoferropyrstherne (Hall, 1981). The generation of similar textures in certain granulites has been attributed to the deformation of orthopyroxene in kink bends (Trommsdorff and

Wenk, 1968; Coe and Muller, 1973; Coe and Kirby, 1975). Orthopyroxene is far more abundant than clinopyroxene, partly reflecting the low Ca content of the rock, and ferro-hornblende is sparse. Evidence of 'retrogression' of the pyroxenes is very rare, although a two-amphibole variety (sample 9) comes from the same locality, signifying the importance of water availability even on a very local scale.

No low-grade assemblages are preserved, but it is probable that the silicate phases originated from the reaction of dolomite/siderite/ankerite- to greenalite/minnesotaite-bearing assemblages with quartz, and the loss of CO_2 from the system (French, 1973; Floran and Papike, 1978; Hall and Goode, 1978). Siderite rich in Mg and Mn has been

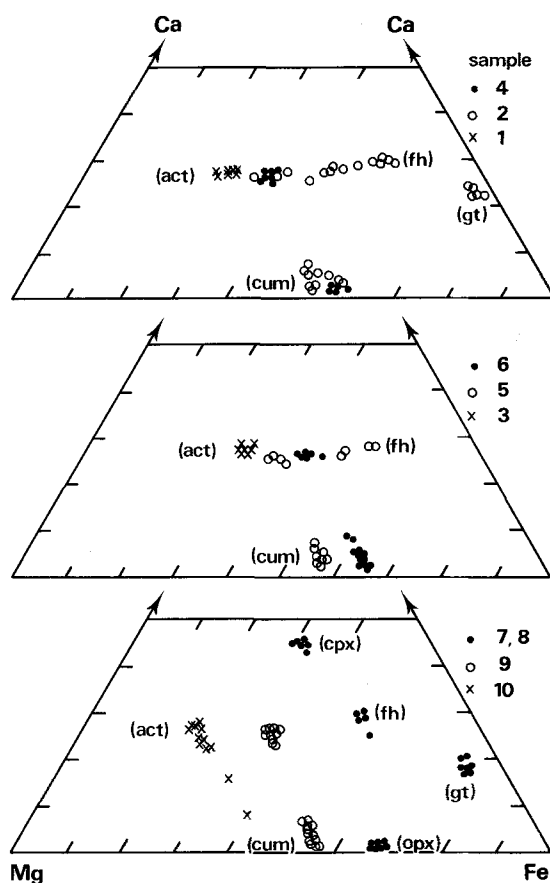


FIG. 3. Ionic Ca:Mg:Fe of coexisting silicate phases in iron-formation samples from Ivisártoq (1-6), Qardlit taserussuat (7-9) and Isukasia (10). Some data omitted for clarity. act: actinolite; cum: cummingtonite; fh: ferro-hornblende; gt: garnet; cpx: clinopyroxene; opx: orthopyroxene. (Fe is Fe^{tot}).

TABLE III. Representative microprobe analyses of cummingtonites

Sample	2	4	5	6	9	10*
SiO ₂	52.86	52.32	52.98	51.95	53.05	55.54
FeO	30.35	31.53	29.94	33.47	29.23	21.84
MnO	2.21	0.70	1.54	0.85	0.93	1.24
MgO	11.84	11.60	12.43	9.92	12.85	16.43
CaO	0.99	0.96	0.97	1.46	1.64	3.41
Total	98.25	97.11	97.87	97.65	97.70	98.45

Number of ions on the basis of 23 oxygens

Si	8.02	8.03	8.02	8.02	8.01	8.06
Fe	3.85	4.01	3.79	4.32	3.69	2.65
Mn	0.28	0.08	0.20	0.11	0.12	0.15
Mg	2.68	2.71	2.81	2.28	2.89	3.55
Ca	0.16	0.15	0.16	0.24	0.27	0.53

* Sample 10 is GGU 213146

TABLE IV. Representative microprobe analyses of actinolites

Sample	1	2	3	4	5	6	9	10
SiO ₂	55.67	51.73	54.57	53.08	53.23	52.56	53.04	56.06
Al ₂ O ₃	0.84	2.52	2.00	0.64	1.39	1.28	1.63	0.61
FeO	13.60	19.27	15.20	19.55	19.80	22.21	18.51	12.55
MnO	0.36	0.63	1.20	0.22	0.59	0.16	0.30	0.29
MgO	15.75	11.48	13.73	12.33	11.59	9.95	12.38	16.62
CaO	11.98	11.35	12.02	10.77	11.14	11.38	11.33	11.78
K ₂ O	-	-	0.08	-	-	-	-	-
Total	98.20	96.97	98.80	96.60	97.74	97.53	97.20	97.91

Number of ions on the basis of 23 oxygens

Si	7.96	7.73	7.85	7.94	7.89	7.90	7.86	7.99
Al	0.14	0.44	0.34	0.11	0.24	0.23	0.28	0.10
Fe	1.63	2.41	1.83	2.45	2.46	2.79	2.29	1.50
Mn	0.04	0.08	0.15	0.03	0.07	0.02	0.04	0.04
Mg	3.36	2.56	2.95	2.75	2.56	2.23	2.73	3.53
Ca	1.84	1.82	1.85	1.73	1.77	1.83	1.80	1.80
K	-	-	0.02	-	-	-	-	-

TABLE V. Representative microprobe analyses of hornblende (h), garnet (g), orthopyroxene (o) and clinopyroxene (c)

Sample	2(h)	5(h)	7(h)	2(g)	7(g)	7(o)	7(c)
SiO ₂	43.07	45.20	41.87	37.48	37.30	49.32	51.01
Al ₂ O ₃	10.02	9.00	15.40	21.29	21.62	0.22	0.38
FeO	28.03	24.05	23.01	31.95	33.09	38.85	18.35
MnO	0.47	0.80	-	1.68	1.18	0.44	0.20
MgO	4.17	7.36	5.23	0.41	1.62	10.18	7.97
CaO	11.15	10.67	10.54	7.74	5.01	0.82	21.08
Na ₂ O	0.58	0.93	0.46	-	-	-	0.38
K ₂ O	0.91	0.63	0.88	-	-	-	-
Total	98.40	98.64	97.38	100.56	100.81	99.83	99.38

Number of ions in formula*

Si	6.74	6.89	6.41	6.01	5.95	2.00	2.00
Al	1.85	1.62	2.78	4.02	4.07	0.01	0.02
Fe	3.67	3.07	2.95	4.28	4.42	1.32	0.60
Mn	0.06	0.10	-	0.23	0.16	0.02	0.01
Mg	0.97	1.67	1.19	0.10	0.38	0.62	0.47
Ca	1.87	1.74	1.73	1.33	1.03	0.04	0.89
Na	0.18	0.28	0.14	-	-	-	0.01
K	0.18	0.12	0.17	-	-	-	-

* on the basis of 23, 24 and 6 oxygens for hornblendes, garnets and pyroxenes respectively.

reported from the Isukaia iron-formation, where both carbonate and silicate-bearing varieties are preserved (Appel, 1980).

Mg-Fe distribution. The principal chemical variables Ca, Mg, and Fe in the coexisting silicate phases are plotted in fig. 3 and representative microprobe analyses are presented in Tables III, IV, and V. The most Mg-rich phases are the actinolites in the banded iron-formation samples (10) from Isukasia, and the single-amphibole assemblage actinolites, which contain magnetite + quartz exsolution (samples 1 and 3). In the other samples actinolite is always more magnesian than coexisting cummingtonite, with $K_{D(\text{Mg})}^{a-c}$ values between 1.05 and 2.1 (Table VI) where $K_{D(\text{Mg})}^{a-c} = [X_{\text{Mg}}^a / (1 - X_{\text{Mg}}^a)] / [X_{\text{Mg}}^c / (1 - X_{\text{Mg}}^c)]$ and X_{Mg} is the mol. fraction Mg/(Mg + Fe²⁺) and the superscripts *a* and *c* refer to actinolite and cummingtonite respectively. In one of the three-amphibole iron-formation samples (sample 2) there is a chemical continuum from the most magnesian actinolite to

the most Al- and Fe-rich ferro-hornblende, with decrease in Mg and Si and corresponding progressive increase in Fe and Al (Tables IV, V). Although Fe³⁺ has not been analysed, the stoichiometry of the microprobe analyses suggests a sequential increase in Fe³⁺ content from zero to approximately 0.4 in the standard formula (based on 23 oxygens) of actinolite to ferro-hornblende respectively, using the method of adjustment of the *C* and *T* site cations (of the general amphibole formula $A_{0-1}B_2C_5T_8O_{22}(\text{OH})_2$) to total 13 by varying the Fe²⁺/Fe³⁺ ratio (cf. Leake, 1978). The maximum value of the Mg-Fe distribution coefficient between actinolite and ferro-hornblende ($K_{D(\text{Mg})}^{a-fh}$) is 4 and 2.3 in samples 2 and 5 respectively, after correction for Fe³⁺ [compared to $K_{D(\text{Mg})}^{a-fh}$ values of 5.2 and 3 for $X = \text{Mg}/(\text{Mg} + \text{Fe}^{\text{Total}})$]. Garnet (Alm₇₀ Gr₂₂ Py₃ Sp₅) is the most Fe-rich silicate phase with a $K_{D(\text{Mg})}^{a-gt}$ value of *c.* 24.5. A summary of the distribution coefficients between the coexisting phases is given in Table VIa.

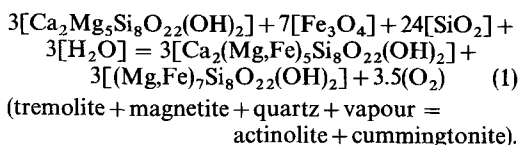
TABLE VI. a) Mg-Fe²⁺ distribution between coexisting amphiboles (and garnet)

Sample	(3,4)	(1,8)	(2,2)	(6,2)
2	rock < actinolite	> cummingtonite	> ferro-hornblende	> almandine
5	(7,2) rock < actinolite	(1,5) > cummingtonite	(1,5) > ferro-hornblende	
4	(9,9) rock < actinolite	(1,8) > cummingtonite		
6	(14,8) rock < actinolite	(1,5) > cummingtonite		
9	(7,1) rock < actinolite	(1,4) > cummingtonite		
1	(13,1) rock < actinolite			
3	(6,7) rock < actinolite			
(General) (rock < actinolite > cummingtonite > ferro-hornblende > almandine)				

TABLE VI. b) Mn distribution between coexisting amphiboles (and garnet)

Sample	(1-1,9)	(2,3-4,7)	(0,8-1,5)
2	almandine > cummingtonite	> actinolite	= ferro-hornblende
5	cummingtonite > actinolite	(1,5-4,0)	(0,5-1,4) = ferro-hornblende
4	cummingtonite > actinolite	(1,9-5,6)	
6	cummingtonite > actinolite	1,8-4,2	
9	cummingtonite > actinolite	1,9-5,6	
(General) almandine > cummingtonite > actinolite = ferro-hornblende			

The paragenesis of the various amphibole assemblages is controlled by many factors, including whole-rock composition, metamorphic grade (P and T), water activity ($a_{\text{H}_2\text{O}}$) and oxygen fugacity (f_{O_2}). The influence of elemental availability is demonstrated by the presence of garnet in the slightly more aluminous samples (2, 3, and 8). The development of cummingtonite is governed in part by the Ca : Mg ratio of the rock (fig. 4). Presumably, available Ca is preferentially incorporated in calcic amphibole (actinolite) formation, which in turn absorbs an appropriate quantity of Mg. Excess Mg may then combine with Fe and Si to form cummingtonite. However, the formation of a more Fe-rich actinolite (e.g. sample 6) in the presence of water releases Mg which becomes available for Ca-poor amphibole:



This reaction predicts an increase in X_{Fe} with increasing cummingtonite : actinolite ratio which is substantiated by the observed mineral assemblages. The most Fe-rich amphiboles ($X_{\text{Mg}}^a = 0.4$) occur in sample 6 which has the lowest modal actinolite/(actinolite + cummingtonite) ratio (0.23), while the most magnesian actinolites ($X_{\text{Mg}}^a = 0.67$) within the samples from Ivisártoq are single-phase amphiboles (figs. 3, 4). These latter amphiboles carry magnetite exsolution lamellae (fig. 2a), suggesting partial dehydration during the (oxidizing) reversal of reaction 1. Thus, while the amphibole compositions do show evidence of the influence of whole-

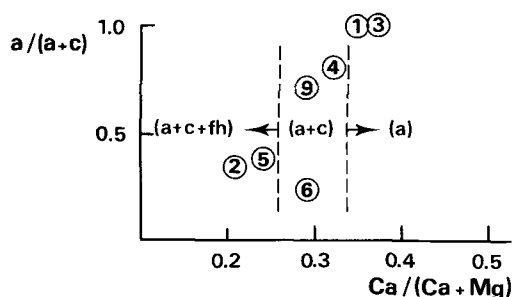
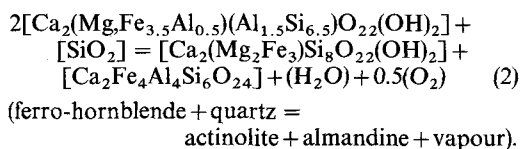


FIG. 4. Modal proportion of actinolite: (actinolite + cummingtonite) ($a/(a+c)$) plotted against $\text{Ca}/(\text{Ca} + \text{Mg})$ (atomic wt. %) in amphibole-bearing iron-formation samples (numbered), showing the apparent chemical boundaries between the single phase actinolite (a), 2-amphibole (actinolite + cummingtonite ($= a+c$)) and 3-amphibole ($a+c+fh$) assemblages (fh = ferro-hornblende). See text for discussion.

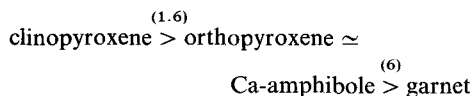
rock composition (cf. Kranck, 1961; Klein, 1966), the $a_{\text{H}_2\text{O}}$ and f_{O_2} states appear to override this parameter to a greater or lesser extent (cf. Popp *et al.*, 1977a, b; Fonarev *et al.*, 1977). Similarly, the development of garnet in two of the samples is partially dependent on composition (Al content), but also signifies a partial dehydration reaction, replacing aluminous amphibole (ferro-hornblende):



This reaction accommodates the observed Mg : Fe and Si : Al variation between the coexisting actinolite-ferro-hornblende series of samples 2 and 5 (fig. 3; Tables IV and V). It is a reducing reaction, evidenced by the apparent relatively higher Fe^{3+} content of the ferro-hornblendes.

Comparison with experimentally determined phase equilibria derived by Cameron (1975), Popp *et al.* (1977a, b), Fonarev *et al.* (1977), and Fonarev and Korolkov (1980) suggest a maximum temperature of around 700 °C at pressures of between 3 and 5 kbar for the formation of the observed composite amphibole-iron-formation assemblages (see Gilbert *et al.*, 1982).

The pyroxene facies iron-formation (sample 7) comprises magnetite + quartz + ferrohypersthene (En_{32}), with minor ferrosalite/ferroaugite (*c.* $\text{Wo}_{45}\text{En}_{25}\text{Fs}_{30}$) and ferro-tschermakitic hornblende (Table V, fig. 3). Almandine garnet ($\text{Alm}_{73}\text{Gr}_{17}\text{Py}_7\text{Sp}_3$) occurs within the pyroxene iron-formation at the contact with an intercalated quartz + almandine lithology (sample 8). Mg-Fe distribution between the silicate phases of this pyroxene-bearing lithology is analogous to that between the various amphiboles. Clinopyroxene has the highest X_{Mg} value (*c.* 0.45) and garnet the lowest (*c.* 0.08). The Mg-Fe distribution between the phases is:

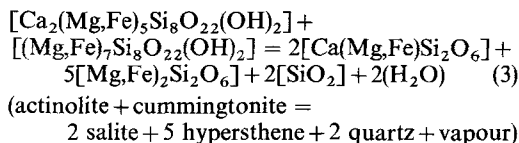


where the numbers are $K_{\text{D}(\text{Mg})}$ values. The stoichiometry of the Ca-amphibole (ferro-tschermakitic hornblende) suggests a Fe^{3+} content of *c.* 0.35 in the amphibole formula (to 23 oxygens). This effects a $\text{Mg}/(\text{Mg} + \text{Fe}^{2+})$ ratio of *c.* 0.37 compared to $\text{Mg}/(\text{Mg} + \text{Fe}^{\text{tot}})$ of 0.28, and changes the orthopyroxene-Ca-amphibole distribution coefficient ($K_{\text{D}(\text{Mg})}^{\text{opx-amp}}$) from 1.2 (Fe^{tot}) to 0.80 (Fe^{2+}).

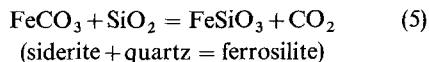
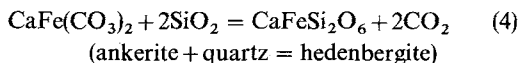
The experimentally determined amphibole-pyroxene equilibria derived by Cameron (1975),

Popp *et al.* (1977a, b), Fonarev *et al.* (1977), and Fonarev and Korolkov (1980) suggest a temperature in excess of 750°C for the pyroxene assemblage. However, the two-pyroxene geothermometer of Lindsley (1983) provides temperature estimates of only 500–600°C and 500–625°C for the formation of the orthopyroxenes and clinopyroxenes respectively in sample 7. The coexisting almandine and ferrosalite (Table V) indicate a metamorphic temperature of c. 625°C according to the garnet-clinopyroxene geothermometer of Ellis and Green (1979). The hornblende-garnet geothermometer of Graham and Powell (1984) gives temperatures of c. 530°C and 600°C for the ferro-tschermakitic hornblende and almandine in this sample, using estimated Fe²⁺ and Fe^{tot.} respectively for the amphibole. However, due to the uncertainty of Fe³⁺ content, the low modal amphibole content and ambiguous textural relationship between the amphibole and garnet, this geothermometer is not considered to be reliable in this case. Similarly, the low Al content of the ferrohystersthene and relatively high Ca content of the almandine put these phases outside the range of most orthopyroxene-garnet geobarometers (e.g. Harley and Green, 1982). The composition of the orthopyroxene (X_{Fe} = 0.68) and absence of fayalite from the assemblage suggest a medium pressure range (5–10 kbar) and a low oxygen fugacity (log₁₀ f_{O₂} = c. –18) (cf. Vaniman *et al.*, 1980; Miyano and Klein, 1983).

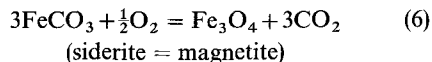
The pyroxene-bearing and amphibole-bearing iron-formation samples (7 and 9) from the Qardlit taserssuat area (fig. 1) were collected from the same locality, signifying the importance and small-scale variability of a_{H₂O}. For equivalent X_{Mg} values of amphiboles and pyroxenes, the pyroxene iron-formation probably developed by a simple dehydration reaction:



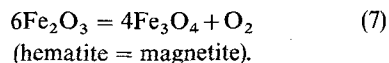
and the Ca-poor:calcic amphibole ratio of 1:1 changes to a Ca-poor:calcic pyroxene ratio of 5:2. The significance of these ratios is discussed below. Whether the contrast in a_{H₂O} between samples 7 and 9 reflects dehydration during metamorphism or a difference in original sedimentary iron-formation facies is uncertain. The most likely anhydrous sedimentary precursor would be a carbonate facies unit:



(cf. Floran and Papike, 1978). During prograde metamorphism, reaction (5) may be preceded by the oxidizing reaction



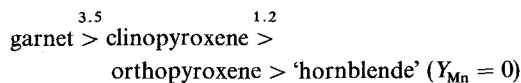
(LaBerge, 1964; French, 1973; Floran and Papike, 1978) which probably coincides with the loss of hematite:



Neither graphite nor any carbonate minerals occur in the pyroxene facies unit (sample 7) and as the intercalated quartz + almandine unit presumably derived from a low-grade hydrous aluminous phase (e.g. chamosite), it seems likely that the amphibole- and pyroxene-bearing assemblages reflect changes in a_{H₂O} during metamorphism.

Manganese distribution. The distribution of Mn between the various silicate phases is somewhat variable (Table VI; fig. 5). The most Mn-rich phase in the amphibole-assemblage rocks is almandine garnet which has a spessartine component of 5 mol. %. The Mn variation within any cummingtonite-actinolite pair is as great as from one pair to another and K_{D(Mn)}^a values range from 1.8 to 5.6, with an average of 3.3 (where K_{D(Mn)}^{c-a} = Y_{Mn}^c/Y_{Mn}^a; Y_{Mn} = Mn/(Mn + Mg + Fe) and c and a refer to cummingtonite and actinolite respectively). Garnet Y_{Mn} values vary from being equal to 1.9 times those of coexisting cummingtonite. The Y_{Mn} of actinolite is broadly equivalent to that of coexisting ferro-hornblende (h) and K_{D(Mn)}^{a-h} values vary from 0.54 to 1.53.

The pyroxene facies iron-formation (sample 7) shows a similar preference of Mn for site occupancy in garnet compared to the coexisting silicate phases (cf. Kretz, 1978). The relationship between Y_{Mn} values for almandine, ferrosalite, ferrohystersthene and ferro-tschermakitic hornblende ('hornblende') in this sample are:



where the numbers are K_{D(Mn)} values. No Mn was detected in the 'hornblende' of this lithology.

Discussion. The observed distribution of Mn in part reflects the substitution of Mn for Fe²⁺ (Mason, 1966; Kranck, 1961). The almandine garnets have the highest X_{Fe} values and correspondingly high Y_{Mn}, while actinolite tends to have the lowest values for these ratios. However, divergence from a simple linear Mn/Fe²⁺ relationship

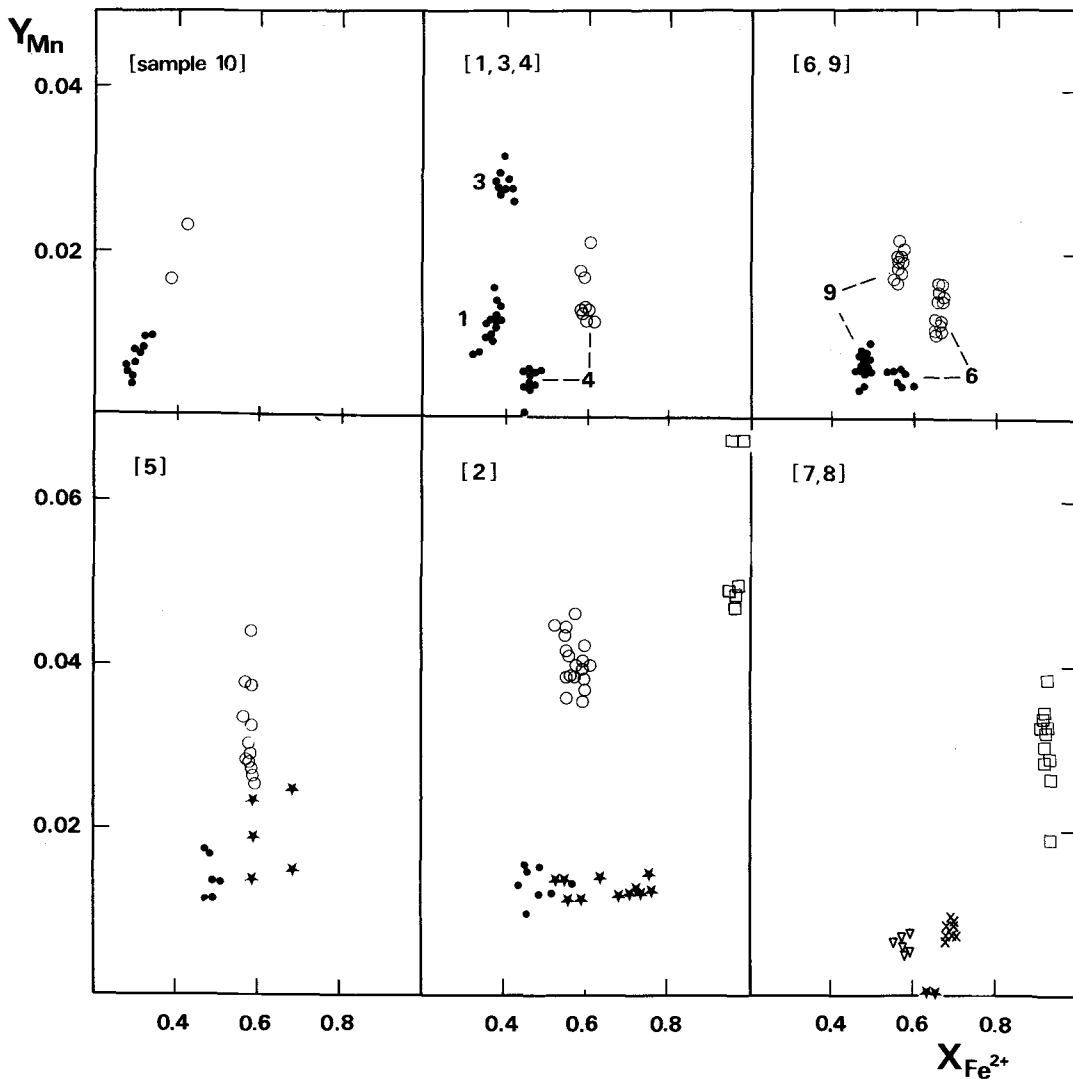


FIG. 5. Summary of Mg-Fe⁽²⁺⁾-Mn distribution between coexisting silicate phases, in amphibole and pyroxene-bearing iron-formation (samples 1 to 10) in terms of Y_{Mn} ($= Mn/(Mn + Mg + Fe^{2+})$) vs. $X_{Fe^{2+}}$ ($= Fe^{2+}/(Mg + Fe^{2+})$). $Fe^{2+} = Fe^{tot}$ for all phases except ferro-hornblende, Fe^{2+}/Fe^{3+} estimated stoichiometrically from microprobe data (cf. Leake, 1978). Symbols: dots, actinolite; open circles, cummingtonite; asterisks, ferro-hornblende; squares, garnet; triangles, clinopyroxene; crosses, orthopyroxene. Several data points omitted for clarity.

appears to result from the interaction of several factors. For example, the more aluminous calcic amphiboles (ferro-hornblendes) have the lowest Mn contents ($= 0$ in sample 7) but have $X_{Fe^{2+}}$ higher than those of coexisting cummingtonite and actinolite. It has been shown (fig. 4) that element availability can strongly influence the proportions of amphiboles present (Ca/Mg and Al partially

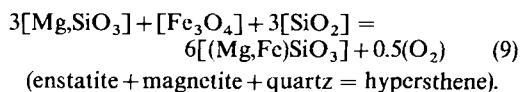
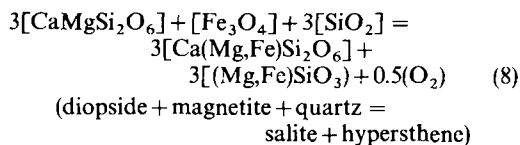
controlling the Ca-poor/calcic amphibole and actinolite/ferro-hornblende ratios respectively). Thus, as Mn demonstrates a clear site occupancy preference for certain phases, the same element availability influences the distribution of a given Mn content in the system. Equally, if a_{H_2O} levels are sufficiently low to promote the formation of garnet in place of hornblende (reaction 2), and, to a lesser

extent, pyroxene in place of amphibole (reaction 3), then contrasting Mn patterns are produced, the formation of garnet or hornblende absorbing or releasing Mn respectively.

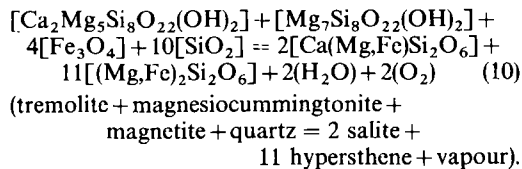
An increase in f_{O_2} also tends to effect a higher Y_{Mn}^a in actinolite in a magnetite buffered system, as this promotes the formation of a more magnesian actinolite at the expense of cummingtonite, releasing Fe to form magnetite (reaction 1). It is significant that the actinolite in one of the single-amphibole samples (3) has the highest observed Y_{Mn} value for actinolite (c. 0.028) and also contains abundant magnetite and quartz exsolution lamellae and 'blebs' (fig. 2c). The difference between the Y_{Mn} of this sample and that of the similar single-amphibole sample (1) is presumably the direct consequence of Mn availability (Table II).

The distribution of Mn in the pyroxene-facies iron-formation unit clearly also depends to a certain extent on f_{O_2} . The partial dehydration reaction (1) from actinolite + cummingtonite to a more magnesian actinolite + magnetite is oxidizing, whereas that from ferro-hornblende to actinolite + garnet (reaction 2) is reducing. The observed pyroxene assemblage in sample 7 has a very high modal orthopyroxene:clinopyroxene ratio (Table II) and the pyroxenes have higher X_{Fe} values than their amphibole equivalents in sample 9 (fig. 3). The composition (X_{Fe}) of pyroxenes is directly related to T and f_{O_2} (and hence f_{H_2O}) conditions (Vaniman *et al.*, 1980; Miyano and Klein, 1983).

Thus, changes in f_{O_2} during the dehydration of amphibole-bearing assemblages (reactions 1 and 3) account for the observed differences in X_{Fe} between the neighbouring amphibole- and pyroxene-iron-formation assemblages. This effects hypothetical redox reactions for pyroxenes equivalent to the amphibole reaction (1):



The dehydrating reaction (3) actinolite + cummingtonite → salite + hypersthene is neutral where the reactants and products have equivalent X_{Mg} values. Combining reactions 3, 8, and 9, the reaction of a cummingtonite + actinolite assemblage to one comprising two pyroxenes with a higher X_{Fe} is both dehydrating and reducing, and invokes the formation of increasingly high modal orthopyroxene:clinopyroxene ratios (= c. 32:1 in sample 7):



Regardless of Si and Fe contents (and excepting sample 8), the various amphibole- and pyroxene-bearing iron-formation rocks are broadly geochemically equivalent and the observed variation in their mineralogy and mineral chemistry can be explained by variations in f_{O_2} and a_{H_2O} :

- (a) dehydration of sample 6 actinolite + cummingtonite → sample 7 pyroxenes (neutral);
- (b) partial dehydration of sample 6 actinolite + cummingtonite → sample 1/3 actinolite + magnetite (oxidizing);
- (c) dehydration of sample 2/4/5 actinolite + cummingtonite → sample 7 pyroxenes (weakly reducing);
- (d) dehydration of sample 2 ferro-hornblende → sample 2 actinolite + garnet (weakly reducing);
- (e) dehydration of sample 1/3 actinolite → sample 7 pyroxenes (reducing);
- (f) dehydration of Isukasia BIF (sample 10) amphiboles → sample 7 pyroxenes (strongly reducing).

Acknowledgements. The samples were collected during field work in 1976 and 1977 by the author under contract to the Geological Survey of Greenland (GGU), except for sample 10 (GGU 213146) which was kindly provided by B. J. Walton. The wet geochemical analysis of the samples by R. Fuge (University College of Wales, Aberystwyth) and L. Shearing (Portsmouth Polytechnic) is gratefully acknowledged. J. V. P. Long is thanked for providing the use of the microprobe facilities at the Department of Earth Sciences, Cambridge University. D. J. Hughes and G. M. Power are thanked for discussion and comment on the manuscript, which is published with the permission of the Director of the Geological Survey of Greenland.

REFERENCES

- Allaart, J. H. (1982) (compiler) 1:500 000 scale geological map Frederikshåb Isblink-Søndre Strømfjord. Geol. Surv. Greenland.
- Appel, P. W. U. (1980) *Precambrian Res.* **11**, 73-87.
- Bayley, R. W., and James, H. L. (1973) *Econ. Geol.* **68**, 934-59.
- Beukes, N. J. (1973) *Ibid.* **68**, 960-1004.
- Bridgwater, D., Keto, L., McGregor, V. R., and Myers, J. S. (1976) In *Geology of Greenland* (A. Escher and S. Watt, eds.). GGU, Copenhagen, 18-75.
- Brown, G. C., Hughes, D. J., and Esson, J. (1973) *Chem. Geol.* **11**, 223-9.
- Cameron, K. L. (1975) *Am. Mineral.* **60**, 375-91.

- Coe, R. S., and Kirby, S. H. (1975) *Contrib. Mineral. Petrol.* **52**, 29-55.
- Coe, R. S., and Muller, W. F. (1973) *Science* **180**, 64-6.
- Dorr, J. V. N. II (1973) *Econ. Geol.* **68**, 1005-22.
- Ellis, D. J., and Green, D. H. (1979) *Contrib. Mineral. Petrol.* **71**, 13-22.
- Floran, R. J., and Papike, J. J. (1978) *J. Petrol.* **19**, 215-88.
- Fonarev, V. I., and Korolkov, G. Y. (1980) *Contrib. Mineral. Petrol.* **73**, 413-20.
- and Dokina, T. N. (1977) *Contrib. Physiochem. Petrol.* **VI**, 224-35.
- French, B. M. (1973) *Econ. Geol.* **68**, 1063-74.
- Fryer, B. J. (1977) *Can. J. Earth Sci.* **14**, 1598-610.
- Gilbert, M. C., Helz, R. T., Popp, R. K., and Spear, F. S. (1982) In *Amphiboles: petrology and experimental phase relations* (D. R. Veblen and P. H. Ribbe, eds.). Mineral. Soc. Am., Washington, 229-353.
- Graham, C. M., and Powell, R. (1984) *J. Metamorphic Geol.* **2**, 13-31.
- Hall, R. P. (1978) *Rapp. Grønlands geol. Unders.* **90**, 57-60.
- (1980) *Ibid.* **97**, 20 pp.
- (1981) Unpubl. Ph.D. thesis, CNA (Portsmouth Polytech.).
- and Friend, C. R. L. (1983) *Geol. J.* **18**, 77-91.
- Hall, W. D. M., and Goode, A. D. T. (1978) *Precambrian Res.* **7**, 129-84.
- Hamilton, P. J., O'Nions, R. K., Bridgwater, D., and Nutman, A. (1983) *Earth Planet. Sci. Lett.* **62**, 263-72.
- Harley, S. L., and Green, D. H. (1982) *Nature*, **300**, 697-701.
- Herrman, A. G. (1970) In *Handbook of geochemistry* II/3 (K. H. Wedepohl, ed.). Springer, New York, 57-71.
- Immega, I., and Klein, C. (1976) *Am. Mineral.* **61**, 1117-44.
- Klein, C. (1966) *J. Petrol.* **7**, 240-305.
- (1968) *Ibid.* **9**, 281-330.
- Kranck, S. H. (1961) *Ibid.* **2**, 137-84.
- Kretz, R. (1978) *J. Geol.* **86**, 599-619.
- Laajoki, K., and Lavikainen, S. (1977) *Bull. Geol. Soc. Finland*, **49**, 105-23.
- La Berge, G. L. (1964) *Econ. Geol.* **59**, 1313-42.
- Leake, B. E. (1978) *Mineral. Mag.* **42**, 533-63.
- Lindsley, D. H. (1983) *Am. Mineral.* **68**, 477-93.
- McGregor, V. R., and Mason, B. (1977) *Am. Mineral.* **62**, 887-904.
- Mason, B. (1966) *Principles of geochemistry*. Wiley, New York, 310 pp.
- Miyano, T., and Klein, C. (1983) *Ibid.* **68**, 699-716.
- Moorbath, S., Allaart, J. H., Bridgwater, D., and McGregor, V. R. (1977) *Nature*, **270**, 43-5.
- Taylor, P. N., and Goodwin, R. (1981) *Geochim. Cosmochim. Acta*, **45**, 1051-60.
- Nutman, A. P., Bridgwater, D., Dimroth, E., Gill, R. C. O., and Rosing, M. (1983) *Rapp. Grønlands geol. Unders.* **112**, 5-22.
- Popp, R. K., Gilbert, M. C., and Craig, J. R. (1977a) *Am. Mineral.* **62**, 1-12.
- (1977b) *Ibid.* **62**, 13-20.
- Robinson, P., Ross, M., and Jaffe, H. F. (1971) *Ibid.* **56**, 1005-41.
- Simmons, E. C., Lindsley, D. H., and Papike, J. J. (1974) *J. Petrol.* **15**, 539-65.
- Taylor, P. N., Moorbath, S., Goodwin, R., and Ptrykowski, A. C. (1980) *Geochim. Cosmochim. Acta*, **44**, 1437-53.
- Taylor, S. R., and McClennan, S. M. (1981) *Spec. Publ. Geol. Soc. Austral.* **7**, 255-61.
- Trommsdorff, V., and Wenk, H. R. (1968) *Contrib. Mineral. Petrol.* **19**, 158-68.
- Turekian, K. K., and Wedepohl, K. H. (1961) *Bull. Geol. Soc. Am.* **72**, 175-92.
- Vaniman, D. T., Papike, J. J., and Labotka, T. (1980) *Am. Mineral.* **65**, 1087-102.
- Wildeman, T. R., and Haskin, L. A. (1973) *Geochim. Cosmochim. Acta*, **37**, 419-38.

[Manuscript received 29 May 1984;
revised 29 September 1984]